

# Flavour specific neutrino self-interaction: $H_0$ tension and IceCube

Arindam Mazumdar<sup>a,\*</sup>, Subhendra Mohanty<sup>b,†</sup>, Priyank Parashari<sup>b,c,‡</sup>

*a)* Centre for Theoretical Studies, Indian Institute of Technology, Kharagpur -721302, India

*b)* Physical Research Laboratory, Ahmedabad- 380009, India

*c)* Indian Institute of Technology, Gandhinagar, 382355, India

## Abstract

Self interaction in the active neutrinos is studied in the literature to alleviate the  $H_0$  tension. Similar self-interaction can also explain the observed dips in the flux of the neutrinos, coming from the distant astro-physical sources, in IceCube detectors. In contrast to the flavour universal neutrino interactions considered for solving the  $H_0$  tension, which is ruled out from particle physics experiments, we consider flavour specific neutrino interactions in CMB and IceCube data. We show that the values of self-interaction coupling constant and mediator mass required for explaining the IceCube dips are inconsistent with the strong neutrino self-interactions preferred by the combination of the HST and Planck data. However, the smaller amount of self-interaction between  $\nu_\tau$  can explain the resonant absorption features in IceCube data and help in solving the  $H_0$  tension.

## 1 Introduction

Self interaction in between the neutrinos has been an active topic of interest in different sectors of cosmology [1–8], astro-physics [9, 10] and laboratory based neutrino experiments [11–13]. In the recent years it has been studied extensively in the context of resolving  $H_0$  tension [3, 4]. Moreover, if this self-interaction is mediated by some MeV scale boson then the resonant on-shell production of mediator in the collision between the astro-physical neutrinos and the cosmic neutrino background can create some signature in the observed IceCube PeV neutrino flux [14–17]. In this paper we check if these two types of applications of self-interaction in neutrinos are consistent with each other or not.

There is a discrepancy between the determination of the Hubble constant  $H_0$  from Planck [18] (which assumes the  $\Lambda$ CDM cosmology) and those from local measurements based on distance ladder and time delay in lensing observations which points to new physics beyond the  $\Lambda$ CDM model [19–22]. The Planck observation finds the value  $H_0 = (67.27 \pm 0.60)$  km/s/Mpc which is in  $4.4\sigma$  disagreement compared for example to the SHOES collaboration [23] determination of  $H_0 = (74.03 \pm 1.42)$  km/s/Mpc, based on the observations by the Hubble Space Telescope of Cepheids in the Large Magellanic Cloud. One of the ways to alleviate the  $H_0$  tension is to have a large self interaction between neutrinos [3]. Self interaction delays the free-streaming of neutrinos and neutrinos cluster at smaller length scales. This is compensated by increasing  $H_0$ . In ref. [3] the best fit value of  $H_0$  which is closer to the distance ladder values was obtained by taking an effective neutrino self-interaction  $\mathcal{L} = G_{\text{eff}}(\bar{\nu}\nu)(\bar{\nu}\nu)$  with  $G_{\text{eff}}$  having two preferred values. The moderate self interaction (MI) with  $\log_{10}(G_{\text{eff}}\text{MeV}^2) = -3.90^{+1.0}_{-0.93}$  and strong self interaction (SI) with  $\log_{10}(G_{\text{eff}}\text{MeV}^2) = -1.35^{+0.12}_{-0.066}$ . In a similar analysis in ref. [4] it is shown that when considering only WMAP data, which measures TT anisotropy spectrum up to multipole  $l \leq 1200$  the bimodal peaks in the probability of  $\log(G_{\text{eff}}\text{MeV}^2)$  disappears and neutrino self interactions are consistent with zero. The bimodal distribution of  $\log(G_{\text{eff}}\text{MeV}^2)$  appears when Planck TT and TE data between  $1200 \leq l \leq 2500$  is included.

In ref. [3] and [4] (and in earlier studies of CMB with neutrino self-interactions [2], [1]) the neutrino self interaction that is considered is identical for all neutrino flavours. It has been pointed out that such large flavour universal couplings of neutrinos which implies mediator masses of  $\mathcal{O}(\text{MeV})$  is severely constrained from particles physics. Strong bounds on  $\nu$  self interactions come from meson decays [12, 24], neutrino-less double beta decay [25] and from  $Z$  and  $\tau$  decays [13]. Neutrino-less double beta decays rule out Majoron mediated  $\nu_e$  interactions as a solution to the  $H_0$  tension [25]. Decays of  $\pi^+/K^+$  to  $e^+\nu_e$  and  $\mu^+\nu_\mu$  put strong constraints on  $\nu_e$  and  $\nu_\mu$  interactions while the  $\nu_\tau$  couplings are only constrained from  $D_s^+ \rightarrow \tau^+\nu_\tau$  which is not so well constrained [12, 24]. The  $Z$  and  $\tau$

\*e-mail: arindam.mazumdar@iitkgp.ac.in

†e-mail: mohanty@prl.res.in

‡e-mail: parashari@prl.res.in

invisible decay width give the strongest bounds for heavy scalar mediators ( $m_\phi > 300\text{MeV}$ ) couplings to  $\nu_\tau$  [13]. To summarise, particle physics allows the self interactions of  $\nu_\tau$  in the MI region ( $m_\phi \sim 10 - 100\text{MeV}$ ) while universal flavour coupling solution considered in [3, 4] as solution to the  $H_0$  tension is ruled out.

In this paper we consider flavour specific self interactions between neutrinos and study their effect of CMB-TT power spectrum. We consider four cases :  $\nu_e, \nu_\mu, \nu_\tau$  and the flavour universal self interactions. From the CMB analysis we find that there is no discernible difference between the  $\nu_\tau$  self interactions allowed from particle physics constraints and the universal flavour interactions. We find like in the earlier papers that  $\log(G_{\text{eff}}\text{MeV}^2)$  has a bimodal distribution in probability with a SI and MI peak in agreement with earlier studies.

Next, we test the flavour specific interactions with IceCube. It has been pointed out that PeV neutrinos from astrophysical sources can interact with cosmic neutrinos and produce an on shell mediator  $\nu\nu \rightarrow \phi$ , when the neutrino energy is  $E_\nu = m_\phi^2/(2m_\nu)$  and neutrino self interactions with MeV mass mediators can have a signature in the neutrino spectrum observed at IceCube [15, 17, 26–30]. The resonant absorption of astrophysical neutrinos will show up as dips in the IceCube flux and this may explain the gap in the IceCube observations between  $E_\nu = 400\text{ GeV} - 1\text{ TeV}$  and the non-observation of Glashow-resonance which is expected at  $E_\nu = 6.3\text{ PeV}$ . Since the neutrino interactions are defined in the flavour basis while the resonance is in the mass basis, the neutrino mixing angles and mass hierarchy plays a crucial role in the IceCube spectrum. We find that all the flavor specific interactions show similar pattern in the IceCube flux data, although these patterns are highly different from the universal interaction. We also find that for the flavor specific and the universal self interaction, the SI region of interaction is ruled out by IceCube data while the MI region is consistent with IceCube for the inverted and normal neutrino mass hierarchy cases.

The paper is organised as follows. In Section 2 we discuss the models of flavour specific self interactions and discuss the scattering cross-section in the low energy limit relevant for CMB anisotropy, neutrino free-streaming and the high energy resonant interactions which are relevant for IceCube neutrinos. In Section 3 we discuss the constraints on effective interaction  $G_{\text{eff}}$  for the four flavour specific interactions from Planck data. In Section 4 we discuss the propagation of high energy neutrinos in cosmic neutrino background with resonant scattering. In Section 5 we apply the analysis of high energy neutrino propagation to IceCube flux considering the four flavour specific neutrino interactions for the two mass hierarchies. In Section 6 we give our conclusions about the viability of neutrino interaction models for solving the  $H_0$  tension in the light of IceCube data.

## 2 Self interaction in neutrinos

Neutrino self interactions can be mediated by scalars and gauge bosons which are motivated from different particle physics models [31–36]. The lepton number is conserved in standard model and in extensions of the standard model where lepton number is broken spontaneously there are scalars called Majorons which arise Goldstone bosons of the lepton number symmetry breaking [37]. Neutrino self interactions can also arise from gauged lepton number and anomaly free extensions of the standard model light gauge bosons which couple to neutrinos and evade all other experimental constraints have been constructed [38]. To analyse the low energy particle physics and CMB constraints its enough to work in the effective theory framework [24]. In order to analyse high energy IceCube interactions where the resonance behaviour of cross section is needed, the full theory is required.

The neutrino self interactions are defined in the flavour basis ( $\nu_\alpha$ ) but the high energy propagation and the neutrino free-streaming is analysed in the neutrino mass basis ( $\nu_i$ ). Here Greek letters are for three different flavors  $e, \mu$  and  $\tau$  and Latin letters are for mass eigenstates and runs from 1 to 3. To relate the couplings in the flavour basis to those in the mass basis the PMNS mixing matrix defined as

$$|\nu_\alpha\rangle = U_{\alpha i}|\nu_i\rangle \quad (1)$$

where, the values of the components of  $U_{\alpha i}$  has been taken from latest NuFit data [39]. Global analysis of the latest neutrino oscillation data provides us the values for all the oscillation parameters like mass squared difference  $\Delta m_{ij}^2 = m_i^2 - m_j^2$  and the mixing angles. However, the existing data failed to give the correct sign of  $\Delta m_{31}^2$  or  $\Delta m_{32}^2$ . Therefore, we have two mass hierarchies namely normal hierarchy (NH) and inverted hierarchy (IH). In case of NH  $m_1 < m_2 < m_3$  and in case of IH  $m_3 < m_1 < m_2$ . For both the hierarchies, we will assume the lowest neutrino mass to be  $m_0$ .

Self-interaction in between the active neutrino species can occur from gauge-interaction or Yukawa like interactions mediated by a scalar( $\phi$ ) particle. In case of Yukawa like interactions the Lagrangian can be written

$$-\mathcal{L} = g_\phi \sum_{\alpha, \beta} g_{\alpha\beta} \phi \bar{\nu}_\alpha \nu_\beta, \quad (2)$$

where  $g_\phi$  is the coupling strength. In the mass basis this can be written as,

$$-\mathcal{L} = g_\phi \sum_{i,j} g_{ij} \phi \bar{\nu}_i \nu_j, \quad (3)$$

where  $g_{ij} = g_{\alpha\beta} U_{\alpha i}^* U_{\beta j}$ . Similarly for gauge-interactions the Lagrangian can be written as

$$-\mathcal{L} = g_X \sum_{\alpha,\beta} \bar{\nu}_\alpha g_{\alpha\beta} \gamma^\mu P_L \nu_\beta X_\mu, \quad (4)$$

where  $g_X$  is the coupling strength. In terms of mass eigenstates this kind of interaction term becomes,

$$-\mathcal{L} = g_X \sum_{i,j} g_{ij} \bar{\nu}_i \gamma^\mu P_L \nu_j X_\mu. \quad (5)$$

The matrix  $g_{\alpha\beta}$  defines the flavour dependence of the interactions. As discussed earlier, in this paper we will work with four different types of flavor dependences. Therefore  $g_{\alpha\beta}$  will be  $\delta_{\alpha\beta}$  for universal interaction and for interaction in a particular flavor it will be a diagonal matrix with only one among  $g_{ee}, g_{\mu\mu}$  or  $g_{\tau\tau}$  set to be one.

For both the scalar and vector exchange cases for momentum-transferred smaller than the mediator mass, the neutrino self-interactions can be described by the four-Fermi term

$$\mathcal{L} = G_{\text{eff}} g_{\alpha\beta} g_{\gamma\delta} \bar{\nu}_\alpha \nu_\beta \bar{\nu}_\gamma \nu_\delta, \quad (6)$$

where  $G_{\text{eff}} = g_\phi^2/m_\phi^2$  or  $G_{\text{eff}} = g_X^2/m_X^2$  for scalar and gauge boson exchange respectively. For the CMB analysis where the momentum transfer in neutrino scatterings are smaller than  $\text{MeV}^2$ , the Four-Fermi effective operator is adequate for the analysis. However when we consider interactions of high-energy astrophysical neutrinos with the cosmic neutrino background, the effective Four-Fermi interaction is not applicable and one must do the calculations for the full theory with the mediator mass playing a crucial role specially near resonant scattering energy. The high energy neutrino-neutrino scattering cross section due to scalar exchange is given by [30, 40, 41],

$$\sigma_{ijkl} = \sigma(\bar{\nu}_i \nu_j \rightarrow \bar{\nu}_k \nu_l) = \frac{1}{4\pi} |g_{kl}|^2 |g_{ij}|^2 \frac{g_\phi^4 s_j}{(s_j - m_\phi^2)^2 + m_\phi^2 \Gamma_\phi^2}, \quad (7)$$

where  $s_i = 2E_i m_i$  and  $\Gamma_\phi = g_\phi^2 \sum_{i,j} |g_{ij}|^2 m_\phi / 4\pi$  is the decay width of the mediator. For vector interactions the cross section has the same Breit-Wigner form with different constants in the prefactor. When summed over the final states this turns out to be

$$\sigma_{ij} = \sigma(\bar{\nu}_i \nu_j \rightarrow \bar{\nu} \nu) = \sum_{k,l} \sigma_{ijkl}. \quad (8)$$

Therefore, we can see that for those energies where  $s_i$  becomes equal to the  $m_\phi^2$  the scattering cross-section becomes maximum. There is a resonant scattering when  $\nu\nu \rightarrow \phi$ . These energies are called resonant energies and denoted by  $E_{Ri} = m_\phi^2 / 2m_i$ . In the section 4 we will show that corresponding to these resonant energy the absorption rate of astrophysical neutrino reaches maximum value and we find the dips in the neutrino spectrum in those energy values.

### 3 Constraints from CMB

We now turn our focus on the cosmological perturbation theory in the presence of self interaction in massive neutrinos. Massive neutrinos play an important role in the evolution of cosmological perturbations as well as in the evolution of background cosmology. Generally, neutrinos free stream in the baryon-photon fluid of early universe and their free streaming length mainly depends on their masses. However, if the neutrinos have self interaction in between them then that reduces their free streaming length and makes the neutrinos clump together more and more than the free neutrinos. The mass of the neutrinos on the other hand not only modifies the free streaming length but also modifies the Hubble parameter. That is why effect of self-interacting neutrino and the effect of massive neutrinos are not same on CMB. The neutrino interactions are defined in the flavor basis while the neutrino density perturbations are analysed in the mass basis. To study this we need to calculate the density matrix for the neutrinos which can be written as  $\rho_{\alpha\beta} = |\nu_\alpha\rangle\langle\nu_\beta|$  and this transforms to mass basis as,

$$\rho_{\alpha\beta} = U_{\alpha i} \rho_{ij} U_{j\beta}^*. \quad (9)$$

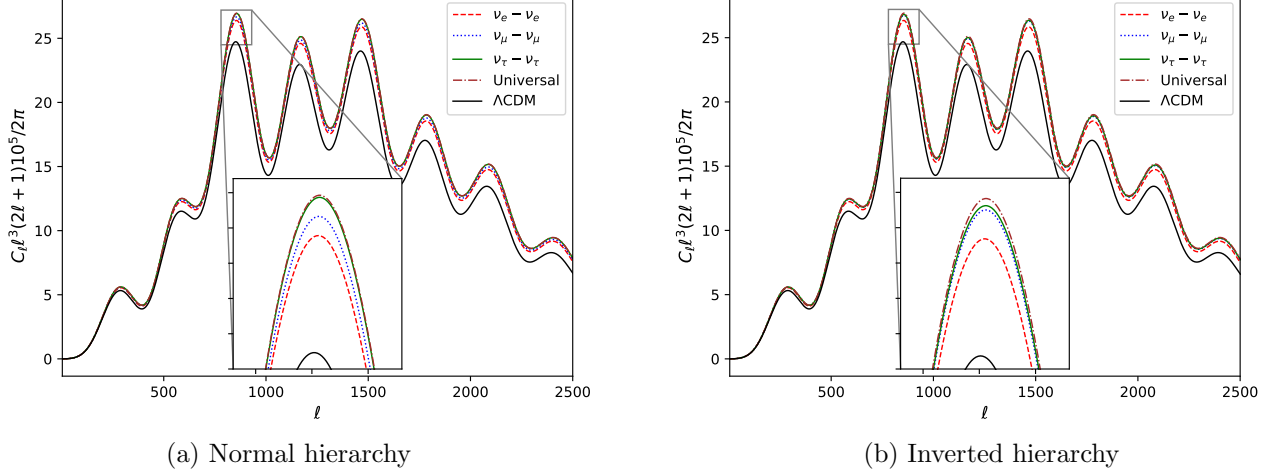


Figure 1: Effects of flavour specific interactions on CMB temperature power spectrum are shown. Power spectrum corresponding to universal interaction almost overlaps with that of  $\nu_\tau$ - $\nu_\tau$  interaction for both the hierarchies. The value of  $G_{\text{eff}}$  has been fixed to  $10^{-1.5}\text{MeV}^{-2}$  for all these cases.

Using this we need to find out the Boltzmann hierarchy equations for the massive neutrinos [42] where the collision term is approximated using relaxing time approximation as [43]

$$\frac{1}{f_0^i} \frac{\partial f_i}{\partial \tau} = -\frac{\Psi}{\tau_\nu}. \quad (10)$$

Here  $\bar{f}_0^i = \sum_\alpha f_0 |U_{\alpha i}|^2 \rho_{\alpha\alpha}$  and  $f_0$  is the zeroth order Fermi-Dirac distribution function [6].  $\Psi$  is the scalar perturbation in the distribution function and  $\tau_\nu$  is the relaxation time which is generally considered as [43]

$$\tau_\nu^{-1} = a n_\nu \langle \sigma v \rangle = \frac{3}{2} \frac{\zeta(3)}{\pi^2} a G_{\text{eff}}^2 T_\nu^5 \rho_{ij}, \quad (11)$$

where  $T_\nu$  is the neutrino temperature and  $a$  is the scale factor. The perturbed Boltzmann equation therefore turns out to be

$$\frac{\partial \Psi_i}{\partial \tau} + i \frac{q(\vec{k} \cdot \hat{n})}{\epsilon} \Psi_i + \frac{d \ln f_0}{d \ln q} \left[ \dot{\eta} - \frac{\dot{h} + 6\dot{\eta}}{2} (\hat{k} \cdot \hat{n})^2 \right] = -\Gamma_{ij} \Psi_j, \quad (12)$$

where  $\Gamma_{ij} = U^\dagger g_{\alpha\beta} U \tau_\nu^{-1}$ . The scalar perturbation  $\Psi$  in distribution function is expanded in terms of Legendre polynomials as,  $\Psi(\vec{k}, \hat{n}, q, \tau) = \sum_{\ell=0}^{\infty} (-i)^\ell (2\ell+1) \Psi_\ell(\vec{k}, q, \tau) P_\ell(\hat{k} \cdot \hat{n})$ . The individual equations corresponding to the multipoles produce the Boltzmann hierarchy equations as follows [44, 45].

$$\dot{\Psi}_{i,0} = -\frac{qk}{\epsilon} \Psi_{i,1} + \frac{1}{6} \dot{h} \frac{d \ln f_0}{d \ln q}, \quad (13a)$$

$$\dot{\Psi}_{i,1} = \frac{qk}{3\epsilon} (\Psi_{i,0} - 2\Psi_{i,2}), \quad (13b)$$

$$\dot{\Psi}_{i,2} = \frac{qk}{5\epsilon} (2\Psi_{i,1} - 3\Psi_{i,3}) - \left( \frac{1}{15} \dot{h} + \frac{2}{5} \dot{\eta} \right) \frac{d \ln f_0}{d \ln q} - \Gamma_{ij} \Psi_{j,2}, \quad (13c)$$

$$\dot{\Psi}_{i,\ell} = \frac{qk}{(2\ell+1)\epsilon} \left[ \ell \Psi_{i,(\ell-1)} - (\ell+1) \Psi_{i,(\ell+1)} \right] - \Gamma_{ij} \Psi_{j,\ell} \quad (\ell \geq 3). \quad (13d)$$

Here, the interaction term in the first two equations eq. (13) was set to zero to conserve the particle numbers and momentum. We modified these equations accordingly in the Boltzmann code CLASS [46] and shown the effects of these interactions on CMB in fig. (1). In general, self interaction between neutrinos helps the small scale perturbations to grow therefore the height of the peaks in CMB power spectrum increases. However, the effect of flavour specific interactions on CMB spectrum shows that there are some minor differences between the effects of

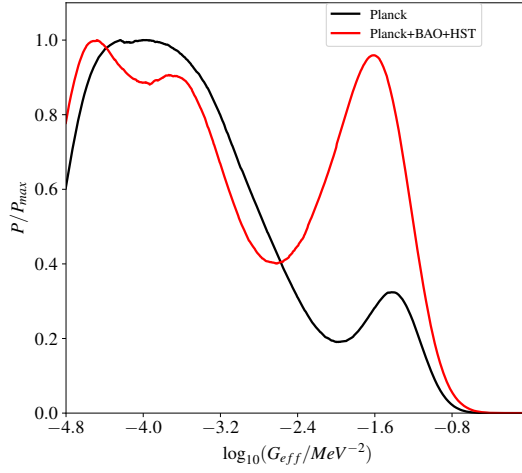


Figure 2: Posterior distribution of  $G_{\text{eff}}$  is bimodal in nature. Inclusion of BAO and HST data increases the probability of  $G_{\text{eff}}$  in strong self interaction region.

different interactions. These effects can be understood from these equations 13. In the case of universal interaction when  $g_{\alpha\beta}$  is equal to  $\delta_{\alpha\beta}$  the  $\Gamma_{ij}$  becomes a diagonal matrix. That means the growth of the scalar perturbation multipoles,  $\Psi_\ell$  of one mass eigenstate depends only on that mass eigenstate. However, for the case of flavour specific interactions growth of  $\Psi_\ell$  depends on other mass eigenstates too. Ultimately, the amount of the effect of self-interaction is determined by the quantity  $\sum_{i,j} \Gamma_{ij}$ . In case of universal interaction it is  $3\tau_\nu^{-1}$ . For  $\nu_e$ - $\nu_e$  interaction this becomes  $2.308 \tau_\nu^{-1}$ , for  $\nu_\mu$ - $\nu_\mu$   $2.643 \tau_\nu^{-1}$  and for  $\nu_\tau$ - $\nu_\tau$  it turns out to be  $2.965 \tau_\nu^{-1}$ . In case of inverted hierarchy these numbers are  $2.309 \tau_\nu^{-1}$  for  $\nu_e$ - $\nu_e$ ,  $2.809 \tau_\nu^{-1}$  for  $\nu_\mu$ - $\nu_\mu$  and  $2.88116 \tau_\nu^{-1}$  for  $\nu_\tau$ - $\nu_\tau$ . Therefore, we see that the effects of universal interaction and  $\nu_\tau$ - $\nu_\tau$  interaction on CMB are indistinguishable in fig. (1).

We proceed to constrain the parameter space of  $G_{\text{eff}}$  with Markov Chain Monte Carlo (MCMC) technique using MontePython [47]. We have used the Planck high- $\ell$  and low- $\ell$  likelihood, following ref [18, 48] where high- $\ell$  consists of only  $TT$  spectrum and  $TT, TE$  and  $EE$  spectrum is incorporated in low- $\ell$  likelihood. In this paper we will call this data set as “Planck”. We have used two other data sets. One is baryon acoustic oscillation scale set by BAO-BOSS data of DR12 release [49] and another one is measured value of  $H_0$  by Hubble space telescope from the observation of Cepheid [23].

As shown in the earlier literature [1–3] we also find that the Planck data prefers a small region of strong interaction between the neutrinos in fig. (2). The posterior of  $G_{\text{eff}}$  is bi-modal. With the inclusion of HST and BAO data the strong interaction part becomes more favorable. The lower value of  $G_{\text{eff}}$  is simply equivalent of  $\Lambda$ CDM cosmology. We did not find any lower cutoff of the  $G_{\text{eff}}$ . The artifact of smaller posterior in the small values of  $G_{\text{eff}}$  is the result of setting hard cutoff of  $10^{-5} \text{MeV}^{-2}$  on the prior by us.

For quantifying the two regions of self-interaction we separate out the points from the posterior distribution which have  $\log_{10}(G_{\text{eff}})$  value greater than -3. We use GetDist [50] to extract the statistics of these peaks. The strong interaction region (we call CMB(SI) onwards) has the value of  $\log_{10}(G_{\text{eff}}/\text{MeV}^{-2})$  in one sigma range as  $-1.68^{+0.46}_{-0.28}$ . The upper bound of  $\log_{10}(G_{\text{eff}}/\text{MeV}^{-2})$  in the mildly interacting region (we call CMB(MI) onwards) is 2.85. The inclusion of HST data and BAO data in the analysis shifts the value of  $H_0$  from  $67.2 \pm 1.8$  (Planck) to  $69.0^{+1.0}_{-0.91}$  (Planck+BAO+HST), which reduces the  $H_0$  tension to some extent.

In fig. (1) we see that difference in between different types of interactions is almost indistinguishable unless magnified. Even after magnification there is almost no difference in between the effects of  $\nu_\tau$ - $\nu_\tau$  and universal interaction on CMB spectra. Therefore, we assume that the MCMC bound on  $G_{\text{eff}}$  for the universal interaction will be applicable to the  $\nu_\tau$ - $\nu_\tau$  interaction for both the hierarchies. With this we move forward to calculate the effect of neutrino self interactions on IceCube flux.

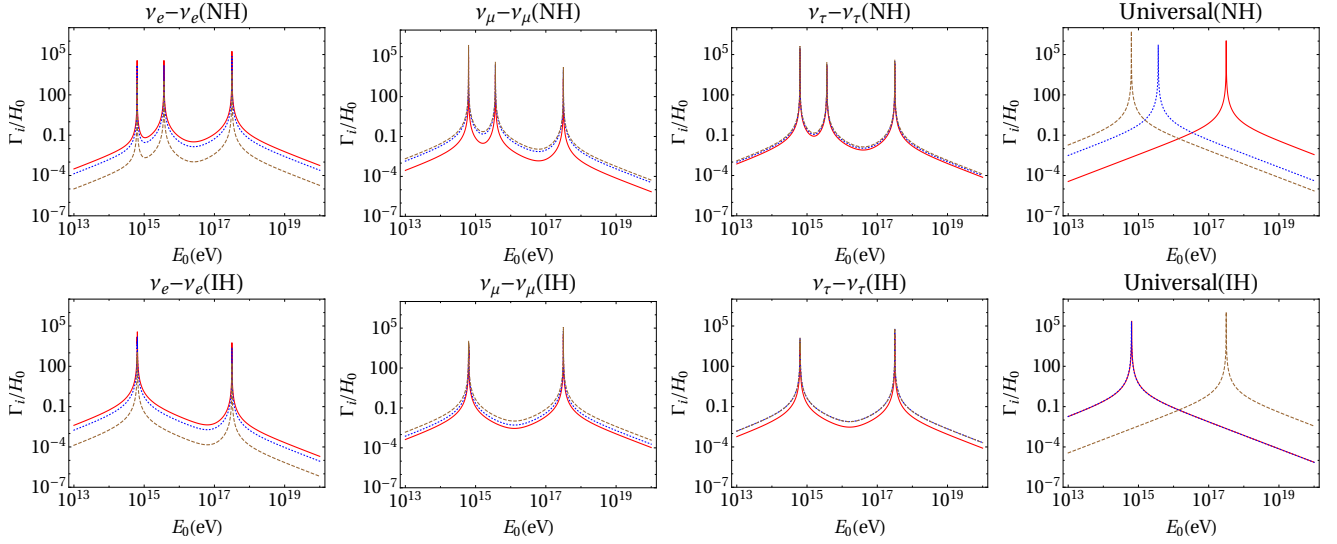


Figure 3: Effect of different types of interactions on absorption rate( $\Gamma_i$ ) is shown. Red, blue (dotted) and brown (dashed) line demonstrate the interaction rates corresponding to mass eigenstates 1,2 and 3 respectively. Here, the upper panel represents normal hierarchy and the lower panel represents inverted hierarchy. Values of the parameters for these plots kept fixed at  $m_\phi = 10^{6.9}$  eV,  $g_\phi = 10^{-1.5}$  and  $m_0 = 10^{-4}$  eV.

## 4 Neutrino absorption by Cosmic Neutrino Background

Propagation of the astrophysical neutrinos in the cosmic neutrino background can be described by the Boltzmann equation. The specific flux  $\Phi_i$  of neutrino mass eigenstates  $m_i$  is defined as

$$\Phi_i = \frac{\partial n_i}{\partial E}, \quad (14)$$

where  $n_i$  is the comoving number density of the astrophysical neutrinos per unit time and  $E$  is the energy of the neutrino mass eigenstates. Therefore, the unit of the  $\Phi_i$  is  $\text{cm}^{-2}\text{s}^{-1}\text{sr}^{-1}\text{eV}^{-1}$ . The Boltzmann equation for  $\Phi_i$  is defined as [14, 41],

$$\frac{\partial \Phi_i}{\partial t} = H\Phi_i + HE\frac{\partial \Phi_i}{\partial E} + S_i(t, E) - \Gamma_i(t, E)\Phi_i + S_{\text{tert},i}(t, E). \quad (15)$$

Here,  $H$  denotes the Hubble parameter,  $S_i$  the source term of the astrophysical neutrinos,  $\Gamma_i$  is absorption rate and  $S_{\text{tert},i}$  is the tertiary source term. Absorption rate  $\Gamma_i = \sum_j \tilde{n}_j \sigma_{ij}$ , where  $\tilde{n}_j$  is the comoving cosmological neutrino number density [30]. Absorption rate is plotted against energy in fig. (3), we can see that  $\Gamma_i$  becomes maximum at the resonance energies. For solving eq. (15), we recast it in redshift( $z$ ) variable as

$$(1+z)\frac{\partial \Phi_i}{\partial z} + E\frac{\partial \Phi_i}{\partial E} = -\Phi_i - \frac{S_i(z, E)}{H} + \frac{\Gamma_i(z, E)}{H}\Phi_i - \frac{S_{\text{tert},i}(z, E)}{H}. \quad (16)$$

Solution of this equation is done using method of auxiliary equation [14, 41], where the auxiliary equation is set to be

$$E = E_0(1+z). \quad (17)$$

Here  $E_0$  denotes the energy of neutrinos at  $z = 0$ . The solution of eq. (16) can be written as [51]

$$\Phi_i(E_0, z) = \int_0^\infty \frac{dz'}{H(z')} \exp \left[ \int_z^{z'} \frac{dz''}{(1+z'')} \frac{\Gamma_i(E, z'')}{H(z'')} \right] \{S_i(E, z) + S_{\text{tert},i}(E, z)\}. \quad (18)$$

The source term  $S_i$  is mainly the astrophysical neutrinos generated from the core-collapsed supernova (CCSN). Therefore this term is taken as [52]

$$S_i(t, E) = R_{\text{CCSN}}(z) \frac{dN_i}{dE} E^{-\gamma}, \quad (19)$$

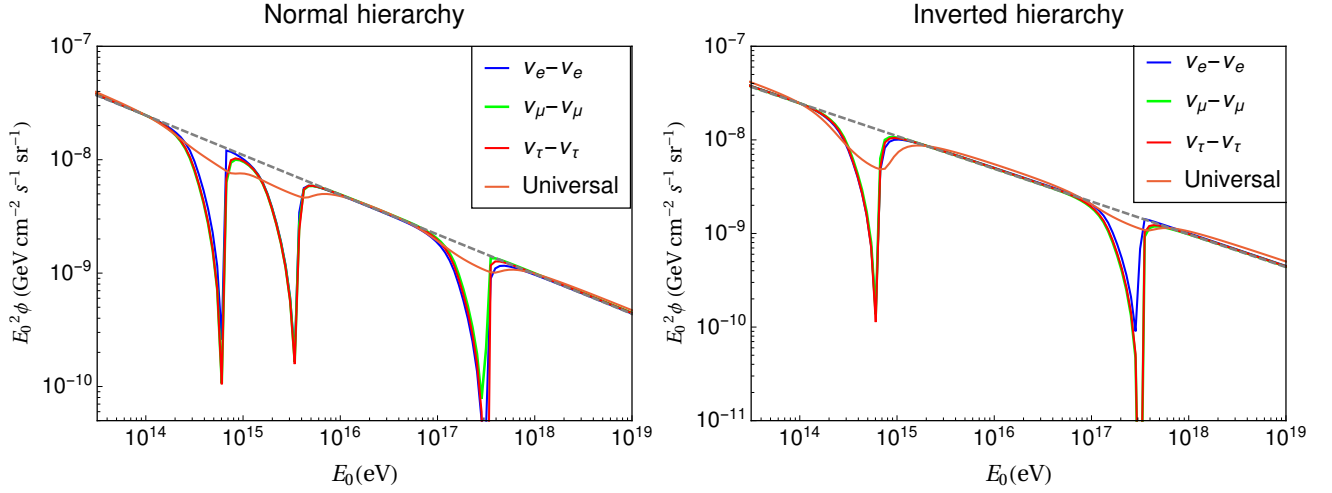


Figure 4: Effects of different types of self interaction on total neutrino flux for both hierarchies are shown within the energy range of interest in IceCube. Values of the parameters for these plots kept fixed at  $m_\phi = 10^{6.9}\text{eV}$ ,  $g_\phi = 10^{-1.5}$ ,  $\gamma = 2.35$  and  $m_0 = 10^{-4}\text{eV}$ . Dashed line corresponds to  $\Phi \propto E_0^{-\gamma}$ .

where  $\frac{dN_i}{dE}$  is the comoving neutrino production rate per unit time per unit energy and it is defined as

$$\frac{dN_i}{dE} = \frac{120E^2 E_{\text{tot}}}{(7\pi^2) 6(k_B T_{\text{sn}})^4 (e^{E/k_B T_{\text{sn}}} + 1)}, \quad (20)$$

where  $E_{\text{tot}} = 1.873 \times 10^{65}\text{eV}$  and  $k_B T_{\text{sn}} = 8\text{ MeV}$  [30].

$R_{\text{CCSN}}(z)$  represents the number density of the core-collapsed supernova as a function of  $z$ . We take this function from ref [53]

$$R_{\text{CCSN}}(z) = \dot{\rho} \left( \left( \frac{z+1}{B} \right)^{\beta\eta} + \left( \frac{z+1}{C} \right)^{\gamma_2\eta} + (z+1)^{\alpha\eta} \right)^{1/\eta} \quad (21)$$

with the parameters being  $\dot{\rho} = 0.0178$ ,  $z_1 = 1$ ,  $z_2 = 4$ ,  $\alpha = 3.4$ ,  $\beta = -0.3$ ,  $\gamma_2 = -3.5$ ,  $\eta = -10$ ,  $B = (z_1 + 1)^{1-\frac{\alpha}{\beta}}$ ,  $C = (z_2 + 1)^{1-\frac{\beta}{\gamma_2}} (z_1 + 1)^{\frac{\beta-\alpha}{\gamma_2}}$ .

Tertiary source term,  $S_{\text{tert},i}$  accounts for the up-scattering of the cosmological neutrinos from the collision with astrophysical neutrinos. This term is approximated in the literature in many different ways. In this paper we use the form provided by ref [30] which is

$$S_{\text{tert},i}(z, E) = \sum_{jkl} (1 + \delta_{il}) \tilde{n}_k(z) \sigma_{jkl} \Phi_j(z, E_{R_k}) \Theta(E_{R_k} - E). \quad (22)$$

We have computed the specific flux of neutrino at  $z = 0$  by numerically solving eq. (18). We have taken the maximum value of  $z$  in this equation to be 10. It is because the  $R_{\text{CCSN}}(z)$  function has non-negligible value up to redshift ten. Normalization of the  $E_0^2 \sum_i \Phi_i$  is fixed to  $2.46 \times 10^{-8} \text{GeV cm}^{-2} \text{s}^{-1} \text{sr}^{-1}$  for neutrino energy equal to 100 TeV [54]. The results for different types of interactions and hierarchies are shown in fig. (4). To understand these plots we have made another set of plots in fig. (3) where the values of absorption rate,  $\Gamma_i$  has been plotted for different interactions. We see that there is a major difference between the universal interaction and the flavour specific interactions. In case of universal interaction the  $g_{ij}$  and  $g_{kl}$  in eq. (7) becomes kronekar delta function and thus  $\Gamma_i$  gets the contribution from  $s_i$  only. However, for flavour specific interactions  $g_{ij}$  mixes all the mass eigenstates and  $s_j$  corresponding to all mass eigenstates contributes in  $\Gamma_i$ . Therefore, in fig. (3) we see that for flavour specific interactions the  $\Gamma_i$  shows resonance peaks in all three possible energy values corresponding to the three mass eigenstates in normal hierarchy. In the case of inverted hierarchy the mass gap between first two mass eigenstates are small, and the peaks corresponding to those mass eigenstates are indistinguishable, therefore, only two peaks are separately visible. These peaks in  $\Gamma_i$  leads to the absorption dips in the flux of astrophysical neutrinos in fig. (4). Since, in the case of flavour specific interactions all mass eigenstates undergo absorption in all dips (three

dips for NH and two dips for IH), we see that the total flux also shows dips in all the resonance energies. However, in the case universal interaction in which energy one mass eigenstate undergoes resonant absorption other mass eigenstates do not. Therefore, in fig. (4) the universal curve shows a more flat line. These three different peaks in the  $\Gamma_i$  of universal interaction can come close together if their mass become degenerate. In that case a prominent dip will be visible in the total neutrino flux for universal interaction also. However, that means it requires a higher value lowest neutrino mass and in the next section we will check if that is consistent with CMB bound.

We found that the contribution of the tertiary source term compared to the core-collapse supernova source term is negligibly small. Moreover, it considerably increases the computation time. Therefore, for constraining the parameter space using IceCube data we neglects the tertiary term in the next section.

## 5 Parameter estimation from flux at IceCube

In IceCube six-year HESE data, 82 events passed the selection criterion of which two are coincident with atmospheric muons and left out. The best fit for single power law flux is [54],

$$E_0^2 \phi = (2.46 \pm 0.8) \times 10^{-8} \left( \frac{E_0}{100 \text{ TeV}} \right)^{-0.92} \text{ GeV cm}^{-2} \text{ s}^{-1} \text{ sr}^{-1} \quad (23)$$

which has softer spectral index than the 3-year ( $\gamma = 2.3$ ) as well as the 4-year ( $\gamma = 2.58$ ) data. These events are binned in 6 values of energy and for other values of energy where no events have been observed upper bounds on the neutrino flux have been provided. For fitting our numerical results of flux with the IceCube data we have solved eq. (18) for 63 different values of  $E_0$  which are equally spaced in log scale within  $E_0$ -range of first 7 points in IceCube data (see fig. (5)). Therefore, we have sampled each energy bin with 9 points in the log scale. The average of these 9 points are assigned as the theoretical prediction of neutrino flux. These theoretical predictions are then compared to the observational values of binned flux and the allowed parameter space ( $m_\phi$ ,  $g_\phi$ ,  $m_0$  and  $\gamma$ ) has been estimated using MCMC technique with Metropolis-Hastings algorithm. Please refer to the appendix A for details.

Before moving forward to describe our findings for different types of interactions and hierarchy let us briefly summarize the effects of different parameters on the features of the specific flux of neutrinos in IceCube. These effects can be listed as

- The higher value of  $m_\phi$  shifts the dips towards the higher values of neutrino energy.
- The higher values of lowest neutrino mass  $m_0$  makes the difference between the neutrino masses smaller and thus makes absorption dips come closer.
- In case of universal interaction higher  $m_0$  makes dips sharper and lower  $m_0$  makes the flux more flat.
- In general, higher value of  $m_0$  makes the neutrinos heavier and therefore the dips move towards lower values of neutrino energy.
- Higher values of  $g_\phi$  make the dips sharper.
- $\gamma$  determines the slope of the flux line. The more  $\gamma$  becomes close to the value 2 the more the flux line becomes flat.

In the next subsections we will discuss our findings of MCMC analysis of parameter space for both the hierarchies and different types of interactions.

### 5.1 Normal hierarchy

**Universal interactions:** Number of visible dips in the flux heavily depends on the value of lowest neutrino mass  $m_0$ . Moreover, as shown in the fig. (4) the universal interaction produces more flat line of specific flux compared to the flavour specific interactions for smaller values of  $m_0$ . However, when the lowest neutrino mass is large, the absorption dips in flux lines corresponding to the different mass eigen states come closer and the dips in the total flux become sharper. Therefore, to fit the dips in the IceCube data the universal interaction prefers a higher value of  $m_0$ . Moreover, CMB also puts a  $1\text{-}\sigma$  upper bound on total neutrino mass allowed in moderately self interacting neutrino case, which is  $\sum m_\nu \leq 0.204 \text{ eV}$  [3]. Using this bound and the best fit values of  $\Delta m_{ij}^2$  from the latest NuFit results [39], we get an upper bound on the lowest neutrino mass to be  $m_0 \leq 0.062$ . In fig. (7) this bound is shown



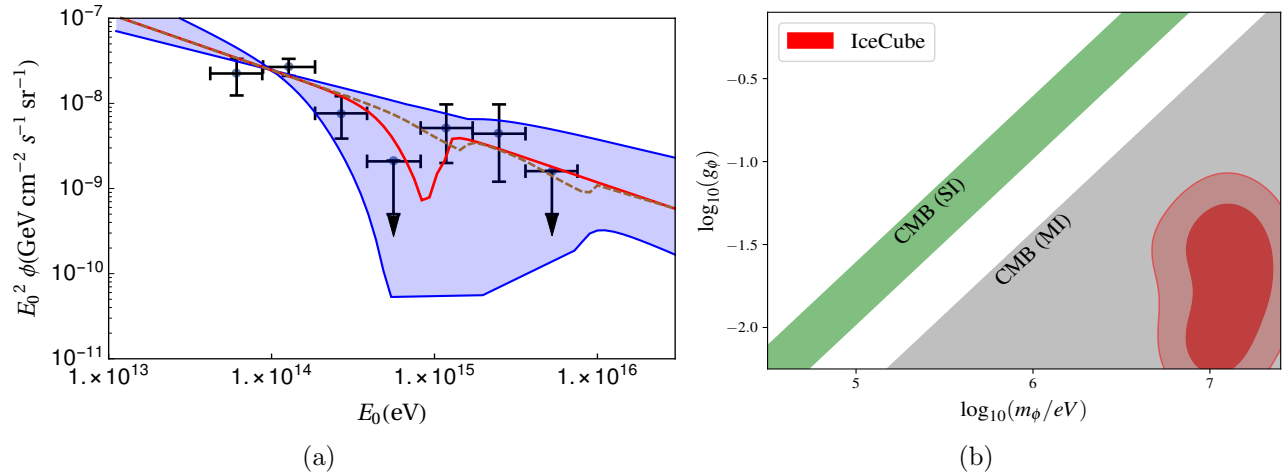


Figure 5: **Universal interaction in normal hierarchy:** (a) The shaded region corresponds to the neutrino flux allowed by the 1- $\sigma$  values of the parameters in the table 1. The values of  $m_\phi, g_\phi$  and  $\gamma$  has been fixed to their bestfit values (in table 1) for both the solid red line and the orange dashed line. However, the solid red corresponds to the maximum  $m_0$  value allowed by CMB and the orange dashed line corresponds to the  $m_0$  value fixed at zero. (b) The allowed region in the  $m_\phi$ - $g_\phi$  plane from IceCube data is shown along with the bounds from the CMB. The allowed region has no overlap with the strong self interaction(SI) band which is favored by inclusion of HST prior with Planck data.

as the green shaded region. Therefore, It is clear from fig. (7) that a substantial region of the preferred mass range by IceCube is disallowed by the CMB bound.

In fig. (5), specific flux in IceCube and the corresponding allowed parameter space for  $m_\phi$ - $g_\phi$  has been shown. The shaded region in the fig. (5)-(a) corresponds to specific flux of the neutrinos by the maximum allowed values of the parameters( $m_\phi, g_\phi, \gamma$ ) within the 1- $\sigma$  range and the maximum allowed value of  $m_0$  within the CMB bound. The shaded region shows that the dip in the specific flux can reach only up to a certain minima and it cannot go dipper cause that will require larger neutrino masses which are disallowed by CMB. We have also plotted a red solid line and a dashed orange line of specific flux. The red solid line corresponds to the maximum allowed value of  $m_0$  to be 0.062eV and the orange line corresponds to the  $m_0 = 0$ eV. Whereas, the values of other parameters  $m_0, g_\phi$  and  $\gamma$  has been fixed to their best-fit values (see table 1). As discussed the previous section, CMB also puts a bound on  $G_{\text{eff}}$ , which translate a bound on  $m_\phi$ - $g_\phi$  parameter space. The bound from CMB for both CMB (SI) and CMB (MI) regime has been shown by the green and gray shaded region respectively in fig. (5)-(b). It is quite evident from fig. (5)-(b) that the IceCube allowed parameter space for  $m_\phi$ - $g_\phi$  is inconsistent with CMB (SI) bound.

**$\nu_\tau$ - $\nu_\tau$  interactions:** The main difference in the features of flavour specific interaction and universal interaction is that while flavour specific interaction can produce two dips to occur at the same time in two different energy bins of IceCube data, the universal interaction allows only one prominent dip. However, the two dips in a flavour specific interaction can be merged to one by increasing the neutrino mass. In fig. (6), specific flux in IceCube and the corresponding allowed parameter space for  $m_\phi$ - $g_\phi$  has been shown. In fig. (6)-(a), we have also plotted two different lines, the solid red and orange dashed line, for specific flux in IceCube which show quite different features. For the orange dashed line,  $m_0$  has been taken to be zero as the lowest possible neutrino mass and all other parameters has been kept at their best fit values. This line can explain two dips in IceCube data at two different energies. If the neutrino mass is increased the orange dashed line in the figure tends towards the solid red line which corresponds to the bestfit values of the all parameters presented in table 1. Therefore we see in the fig. (6)-(a) that the solid red line and the orange dashed line represent the one and two dip solutions in the IceCube energy range. Again the shaded region in the fig. (6)-(a) corresponds to specific flux of the neutrinos by the maximum allowed values of the parameters( $m_\phi, g_\phi, \gamma$ ) within the 1- $\sigma$  range and the maximum allowed value of  $m_0$  within the CMB bound. Similar to the universal case, it is quite evident from fig. (6)-(b) that the IceCube allowed parameter space for  $m_\phi$ - $g_\phi$  is inconsistent with CMB (SI) region.

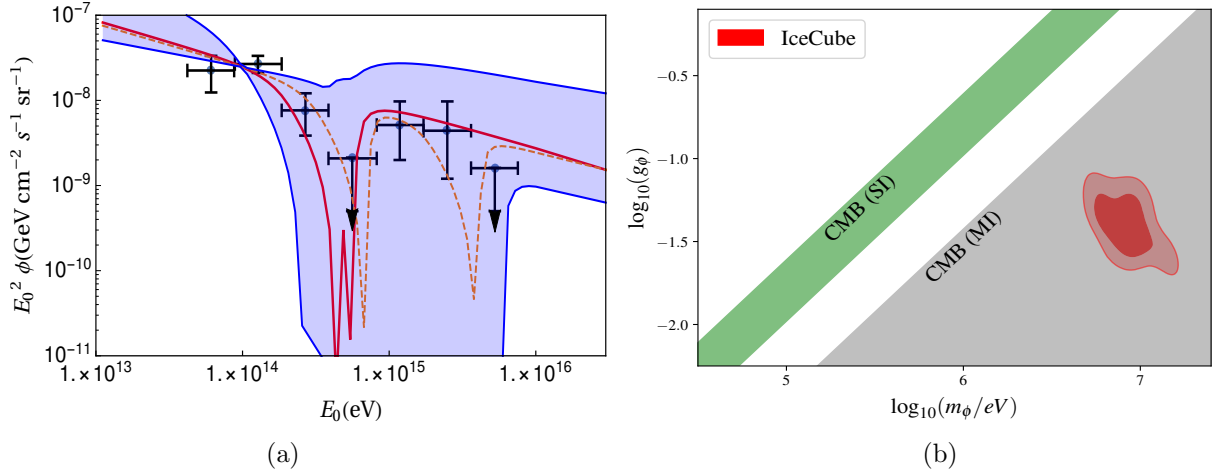


Figure 6:  $\nu_\tau$ - $\nu_\tau$  **interaction in normal hierarchy**: (a) The shaded region corresponds to the neutrino flux allowed by the 1- $\sigma$  values of the parameters in the table 1. The solid red line correspond to the best fit values of the parameters and the orange dashed line corresponds to the best fit value of  $m_\phi, g_\phi$  and  $\gamma$  (in table 1) and the value of  $m_0$  is fixed at zero. (b) The allowed region in the  $m_\phi$ - $g_\phi$  plane from IceCube data is shown along with the bounds from the CMB. The allowed region has no overlap with the strong self interaction(SI) band.

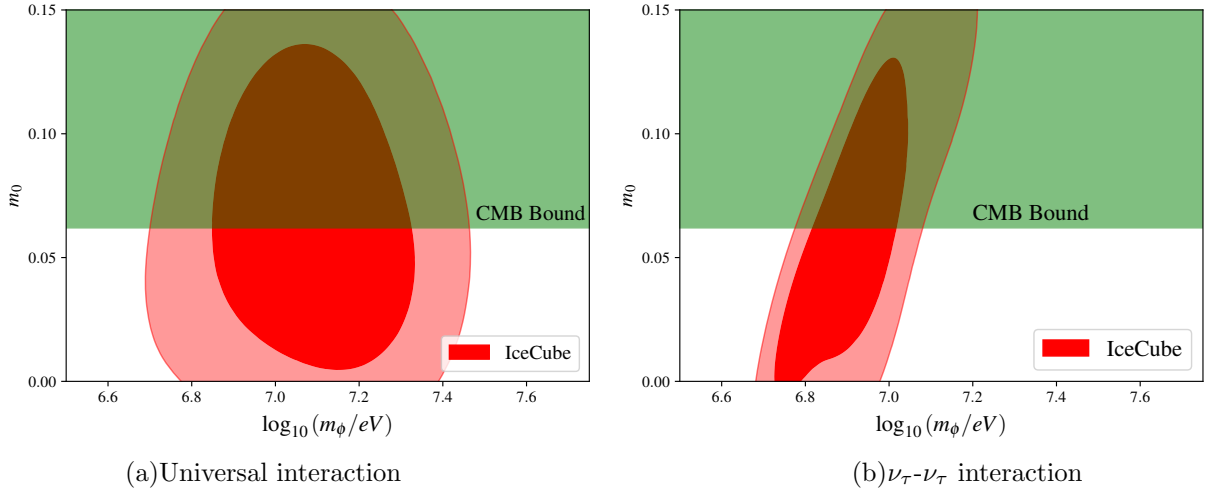


Figure 7: The green region shows the values of minimum neutrino mass( $m_0$ ) excluded by CMB(Planck) data for normal hierarchy. A major portion of the preferred values by IceCube data is disfavored by CMB.

Parameter	68% limits
<b>Universal interaction</b>	
$m_0(\text{eV})$	$0.067^{+0.038}_{-0.046}$
$\log_{10}(m_\phi/\text{eV})$	$7.09 \pm 0.15$
$\log_{10} g_\phi$	$-1.75 \pm 0.31$
$\gamma$	$2.66^{+0.21}_{-0.18}$
<b><math>\nu_\tau</math>-<math>\nu_\tau</math> interaction</b>	
$m_0(\text{eV})$	$0.062^{+0.042}_{-0.046}$
$\log_{10} m_\phi/\text{eV}$	$6.92 \pm 0.11$
$\log_{10} g_\phi$	$-1.40 \pm 0.13$
$\gamma$	$2.50 \pm 0.17$

Table 1: Allowed parameters with IceCube data for normal hierarchy.

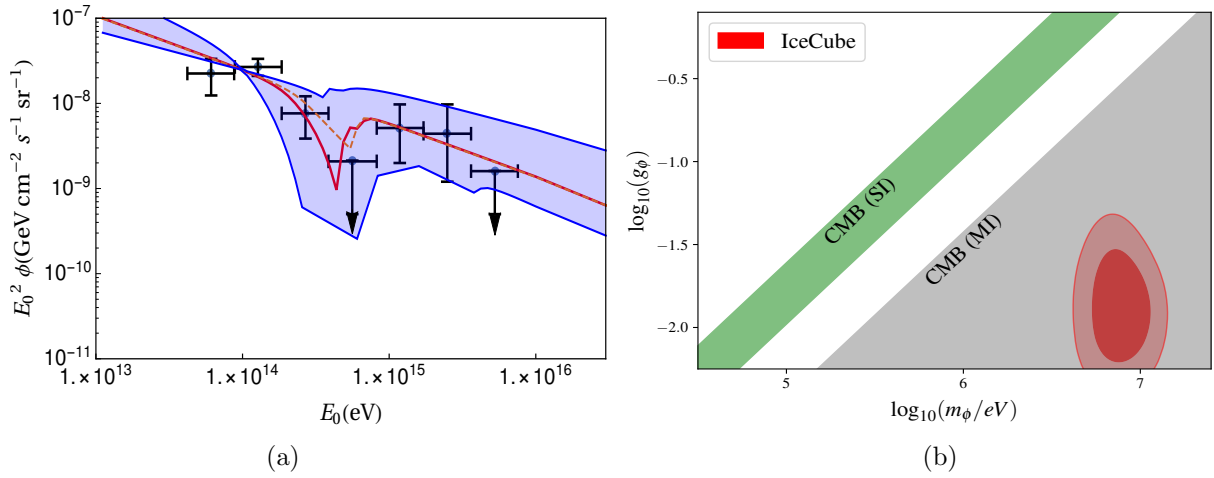


Figure 8: **Universal interaction in inverted hierarchy:** (a) The shaded region corresponds to the neutrino flux allowed by the  $1\text{-}\sigma$  values of the parameters in the table 2. The solid red line correspond to the best fit values of the parameters and the orange dashed line corresponds to the best fit value of  $m_\phi, g_\phi$  and  $\gamma$  (in table 2) and the value of  $m_0$  is fixed at zero. (b) The allowed region in the  $m_\phi\text{-}g_\phi$  plane from IceCube data is shown along with the bounds from the CMB. The allowed region has no overlap with the strong self interaction(SI) band.

## 5.2 Inverted Hierarchy

**Universal interactions:** Similar to the case of normal hierarchy, in the case of inverted hierarchy, the universal interaction produces a flatter specific flux line compared to the the flavour specific interactions for smaller values of  $m_0$  as well. Since large value for  $m_0$  makes masses of mass eigenstates almost same, we get a single dip solution for such case. Therefore, again to fit the dips in the IceCube data the universal interactions prefers a higher value of  $m_0$ . Again, like the normal hierarchy case, CMB also put a bound on the lowest neutrino mass  $m_0 \leq 0.054$  eV which comes from the  $\sum m_\nu \leq 0.204$  eV for moderate self-interaction [3]. Therefore, a substantial region of the preferred mass range by IceCube is disallowed by the CMB bound (see fig. (10)).

In fig. (8), specific flux in IceCube and the corresponding allowed parameter space for  $m_\phi\text{-}g_\phi$  has been shown. The shaded region in the fig. (8)-(a) corresponds to specific flux of the neutrinos for the maximum allowed values of the parameters( $m_\phi, g_\phi, \gamma$ ) within the  $1\text{-}\sigma$  range and the maximum allowed value of  $m_0$  within the CMB bound. Similar to the normal hierarchy case, the shaded region shows that the dip in the specific flux can reach only up to a certain minima and it cannot go deeper cause that will require larger neutrino masses which are disallowed by CMB. We have also plotted a red solid line and a dashed orange line of specific flux. The red solid line corresponds to the best fit values of all the parameters listed in table 2. Whereas, the orange line corresponds to the  $m_0 = 0\text{eV}$  and all other parameters fixed at their best fit values. Similar to the normal hierarchy, It is quite evident from fig. (8)-(b) that the IceCube allowed parameter space for  $m_\phi\text{-}g_\phi$  is inconsistent with CMB (SI) bound.

Parameter	68% limits
<b>Universal interaction</b>	
$m_0(\text{eV})$	$0.052^{+0.034}_{-0.040}$
$\log_{10}(m_\phi/\text{eV})$	$6.883 \pm 0.091$
$\log_{10} g_\phi$	$-1.87 \pm 0.20$
$\gamma$	$2.63 \pm 0.17$
<b><math>\nu_\tau\text{-}\nu_\tau</math> interaction</b>	
$m_0(\text{eV})$	$0.062^{+0.038}_{-0.058}$
$\log_{10}(m_\phi/\text{eV})$	$6.936^{+0.089}_{-0.14}$
$\log_{10} g_\phi$	$-1.25 \pm 0.17$
$\gamma$	$2.46^{+0.18}_{-0.16}$

Table 2: Allowed parameters with IceCube data for inverted hierarchy.

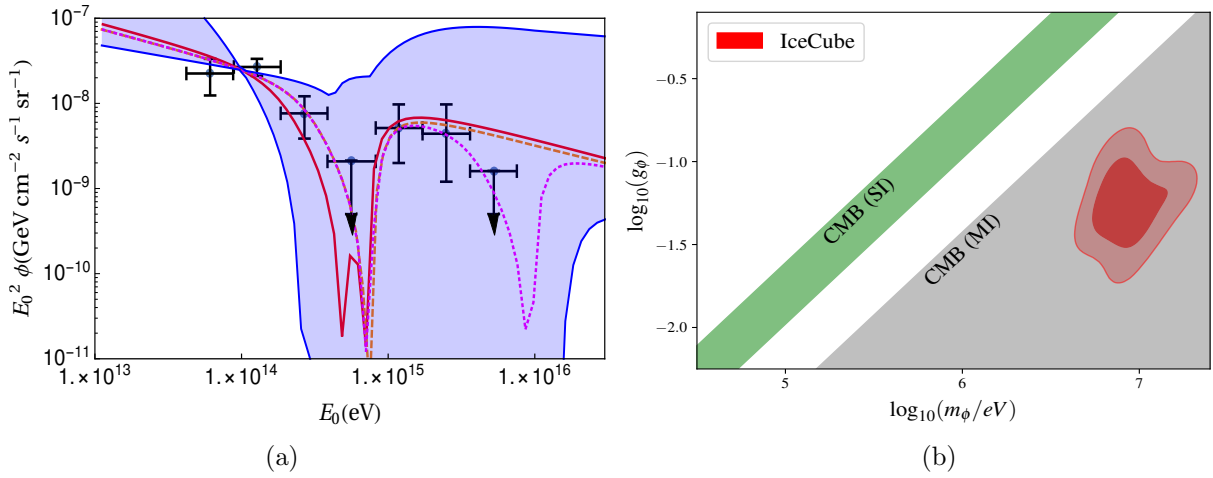


Figure 9:  $\nu_\tau$ - $\nu_\tau$  **interaction in inverted hierarchy:** (a) The shaded region corresponds to the neutrino flux allowed by the 1- $\sigma$  values of the parameters in the table 2. The values of  $m_\phi$ ,  $g_\phi$  and  $\gamma$  has been fixed to their bestfit values (in table 2) for all the solid red line, orange dashed line and the pink dotted line. However, the solid red line corresponds to the maximum value of  $m_0$  allowed by CMB; the orange dashed line corresponds to the  $m_0$  value fixed at zero and the pink dotted line corresponds to the lowest 1- $\sigma$  allowed value of  $m_0$ . (b) The allowed region in the  $m_\phi$ - $g_\phi$  plane from IceCube data is shown along with the bounds from the CMB. The allowed region has no overlap with the strong self interaction(SI) band.

**$\nu_\tau$ - $\nu_\tau$  interactions:** In case of inverted hierarchy, for the  $\nu_\tau$ - $\nu_\tau$  interactions, number of dips in the IceCube energy range depends on the  $m_0$  value. For very small  $m_0$  value (close to zero) we get only dip in the IceCube energy range. However, in case of larger  $m_0$  value for which all the three mass eigenstates come close we also find only dip in the IceCube energy range. On the other hand, for  $m_0$  value not very close to zero and also not very large enough to make all three mass eigenstates degenerate, we can get two dip solution in the IceCube energy range. In fig. (9), specific flux in IceCube and the corresponding allowed parameter space for  $m_\phi$ - $g_\phi$  has been shown. In fig. (9)-(a), we have also plotted three different lines, the solid red, orange dashed and dotted pink line, for specific flux in IceCube which shows very different features. The pink dotted line is for  $m_0 = 0$  eV and all other parameters fixed at their best fit values (see table 2). We can see from the fig. (9)-(a) that this line represent one dip solution. As we increase the  $m_0$  values to the best fit value given in table 2, the pink dotted line tend towards the orange dashed line for which all other parameters has been kept at their best fit values. Again it is clear from fig. (9)-(a) that this line can explain two dips in IceCube data at two different energies. If the neutrino mass is increased further the orange dashed line in the figure tends towards the solid red line which corresponds to the bestfit values of the all parameters presented in table 2 except  $m_0$  which is kept at the CMB allowed maximum value. Therefore we see in the fig. (9)-(a) that both the solid red line and orange dashed line represent the one dip solutions in the IceCube energy range, whereas the pink dotted line represents the two dip solution in the IceCube energy range. Again the shaded region in the fig. (9)-(a) corresponds to specific flux of the neutrinos by the maximum allowed values of the parameters( $m_\phi$ ,  $g_\phi$ ,  $\gamma$ ) within the 1- $\sigma$  range and the maximum allowed value of  $m_0$  within the CMB bound. Similarly like the universal case, It is quite evident from fig. (9)-(b) that the IceCube allowed parameter space for  $m_\phi$ - $g_\phi$  is inconsistent with CMB (SI) bound.

## 6 Conclusions

In this paper we have studied the self-interaction in between the neutrinos in the context of  $H_0$  tension and the observed dips in the neutrino flux of IceCube. We have shown that the flavour specific interaction and the universal interaction does not affect CMB power spectrum very much differently. Even the inverted hierarchy and the normal hierarchy do not have much distinguishable effect. The bound on the self interaction parameter  $G_{\text{eff}}$  from the Planck data shows a bimodal feature in its distribution which is consistent with the earlier studies. This bimodal nature even gets magnified in the case of joint analysis with Planck, BAO and HST data. Moreover, in this case, the value of  $H_0$  moves upward from  $67.2 \pm 1.8$  (Planck) to  $69.0^{+1.0}_{-0.91}$  (Planck+BAO+HST).

However, the effect of flavour specific and universal interaction on the total flux of astrophysical neutrinos in

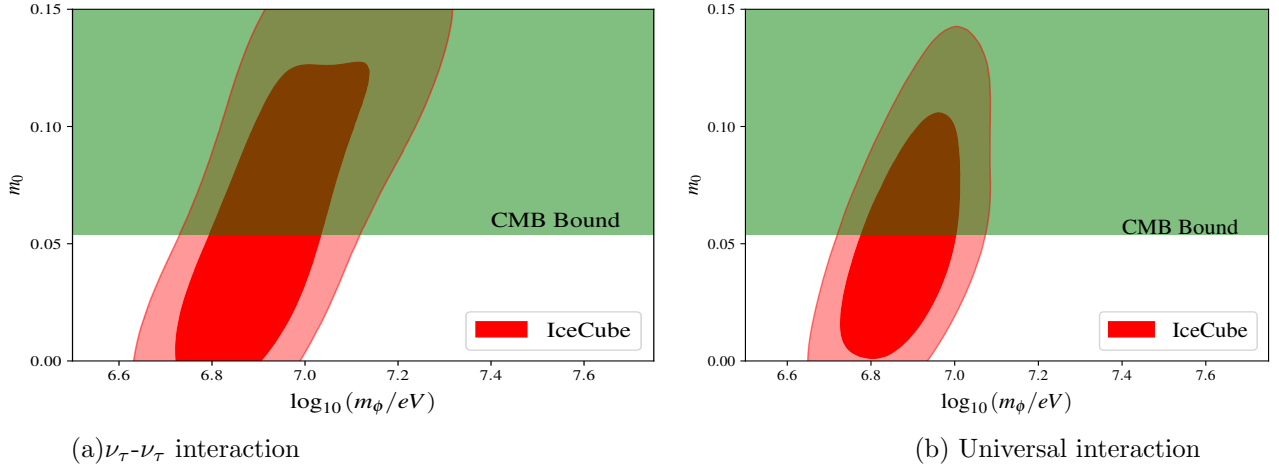


Figure 10: The green region shows the values of minimum neutrino mass( $m_0$ ) excluded by CMB(Planck) data for inverted hierarchy. In both the cases a significant portion of the preferred  $m_0$  values by IceCube data is excluded by the CMB bound.

IceCube is quite different. We have plotted different ways of fitting IceCube data with these interactions and constrained the parameter space of self-interaction mediator and the neutrino mass. We find that the dips at around 550 TeV and at around  $5 \times 10^3$  TeV (which shows the non-appearance of Glashow resonance) can be simultaneously explained using the neutrino self interaction in flavour specific cases. However, in case of universal interaction it is impossible to explain two dips simultaneously. By adjusting the parameters one dip can occur at one position only in case of universal interaction. Moreover, by suitably adjusting the lowest neutrino mass two different dips in flavor specific neutrino cases can also be merged to a single dip. We find that there is no distinguishable difference in the features of neutrino flux line for  $\nu_e$ - $\nu_e$ ,  $\nu_\mu$ - $\nu_\mu$  and  $\nu_\tau$ - $\nu_\tau$  interaction. Therefore, all our analysis and results presented for the  $\nu_\tau$ - $\nu_\tau$  interaction is equally applicable to the  $\nu_e$ - $\nu_e$  and  $\nu_\mu$ - $\nu_\mu$  interaction cases. There is one more finding in our analysis, that is, in case of universal interaction, CMB upper bound on neutrino masses restricts the depth of the dips at resonance energies. So far our allowed depth of the dips are still consistent with the CMB bound. But if in future there is even more suppression in the absorption regions of the IceCube data then that might invalidate universal interaction completely.

Hierarchy also plays an important role in determining the position and the shape of the absorption dips in the neutrino flux at IceCube. In case of universal interaction and normal hierarchies two very small dips can occur for lowest neutrino mass being zero. However, for the same case in inverted hierarchy there can be only one small dip if  $m_0$  fixed at zero. In case of  $\nu_\tau$ - $\nu_\tau$  interaction, normal hierarchy can produce two dips in the above mentioned two energy values with zero value of  $m_0$ . However, in case of inverted hierarchy that same feature requires small but non zero lowest neutrino mass.

Since, the value of mediator mass( $m_\phi$ ) changes the position of the dips and the value of the interaction strength ( $g_\phi$ ) changes the sharpness of the dips, the MCMC analysis provide quite strict bound on those values. Larger values of  $g_\phi$  beyond the obtained bound can produce sharper dips in the resonance energies, but it will not be able to explain the absorption feature throughout the specified energy range of a certain bin in the IceCube data. We found that the CMB bound on the neutrino self interaction parameters in strong interaction region, which are inferred from the joint analysis of Planck, HST and BAO data, are inconsistent with the parameter space inferred from the IceCube data. This means that there can be only moderate self-interaction in between the neutrinos which can produce an effect on IceCube flux. We have also shown the allowed region of flux line beyond 10 PeV neutrino energy in our results. Therefore, it serves as a prediction for upcoming data in IceCube experiment in ultra high energies.

## Acknowledgment

We acknowledge the computation facility, 100TFLOP HPC Cluster, Vikram-100, at Physical Research Laboratory, Ahmedabad, India.

# Appendix

## A Numerical details

The MCMC analysis performed in the paper for the IceCube data is based upon the Metropolis-Hastings algorithm [55]. The likelihood function used in the analysis assumes a generalized likelihood function for asymmetric error, following ref. [56] which can be written as

$$\ln[L] = -\frac{1}{2} \left( \frac{\hat{x} - x}{\sigma + \sigma'(\hat{x} - x)} \right)^2, \quad (24)$$

where,

$$\sigma = \frac{2\sigma_+\sigma_-}{\sigma_+ + \sigma_-} \text{ and } \sigma' = \frac{\sigma_+ - \sigma_-}{\sigma_+ + \sigma_-} \quad (25)$$

In case of symmetric errors  $\ln[L]$  turns out to be  $-\chi^2$ . In the likelihood function we used the binned flux data of ref. [54] as observational values. Theoretical values are calculated from the solution of eq. (18) for 63 different points in the IceCube energy range where we have taken 9 points from each bin in equally spaced log space of  $E_0$ .

We have used the Gaussian priors for the parameters and the corresponding values are given table 3. We have also put hard cutoff on the maximum and minimum values at 7.4 and 6.2 respectively for  $\log_{10}(m_\phi/\text{eV})$ . Lowest neutrino mass  $m_0$  has also been assigned with maximum and minimum values of 0.15 eV and 0 respectively.

Parameter	mean	1- $\sigma$
$m_0(\text{eV})$	0.05	0.02
$\log_{10}(m_\phi/\text{eV})$	6.7	0.05
$\log_{10} g_\phi$	-1.5	0.05
$\gamma$	2.35	0.05

Table 3: Priors used in MCMC with IceCube data

The cosmological parameters of interest in this paper are the six standard cosmological parameters and one parameter related to self interacting neutrinos( $G_{\text{eff}}$ ). The six standard cosmological parameters are: the fraction density of cold dark matter and baryonic matter at present multiplied by square of the reduced Hubble parameter ( $\omega_{\text{cdm}}$  and  $\omega_b$  respectively), acoustic scale of baryon acoustic oscillation ( $\theta_s$ ), amplitude and the spectral index of the primordial density perturbations ( $A_s$  and  $n_s$  respectively) and optical depth to the epoch of re-ionization ( $\tau_{\text{reio}}$ ). Seven parameters have been varied in this analysis and the corresponding priors for these parameters are given in table 4. We have given Gaussian prior for our purpose. In case of  $\log_{10} G_{\text{eff}}$ , we have assigned the maximum and minimum values -5.0 and -0.1 respectively. Lowest neutrino mass  $m_0$  has been kept fixed at 0.0001 and a minimum value of  $\tau_{\text{reio}}$  was specified to be 0.04.

Parameter	mean	1- $\sigma$
$\omega_b$	$2.2377 \times 10^{-2}$	$0.015 \times 10^{-2}$
$\omega_{\text{cdm}}$	0.12010	0.0013
$100\theta_s$	1.04110	3e-4
$\ln 10^{10} A_s$	3.0447	0.015
$n_s$	0.9659	0.0042
$\tau_{\text{reio}}$	0.0543	0.008
$\log_{10} G_{\text{eff}}$	-1.5	0.2

Table 4: Priors used in MCMC with Planck, BAO and HST data.

## References

- [1] L. Lancaster, F.-Y. Cyr-Racine, L. Knox, and Z. Pan, *A tale of two modes: Neutrino free-streaming in the early universe*, *JCAP* **07** (2017) 033, [[arXiv:1704.06657](#)].

- [2] I. M. Oldengott, T. Tram, C. Rampf, and Y. Y. Wong, *Interacting neutrinos in cosmology: exact description and constraints*, *JCAP* **11** (2017) 027, [[arXiv:1706.02123](#)].
- [3] C. D. Kreisch, F.-Y. Cyr-Racine, and O. Doré, *Neutrino puzzle: Anomalies, interactions, and cosmological tensions*, *Phys. Rev. D* **101** (2020), no. 12 123505, [[arXiv:1902.00534](#)].
- [4] M. Park, C. D. Kreisch, J. Dunkley, B. Hadzhiyska, and F.-Y. Cyr-Racine,  *$\Lambda$ CDM or self-interacting neutrinos: How CMB data can tell the two models apart*, *Phys. Rev. D* **100** (2019), no. 6 063524, [[arXiv:1904.02625](#)].
- [5] G. Barenboim, P. B. Denton, and I. M. Oldengott, *Constraints on inflation with an extended neutrino sector*, *Phys. Rev. D* **99** (2019), no. 8 083515, [[arXiv:1903.02036](#)].
- [6] A. Mazumdar, S. Mohanty, and P. Parashari, *Inflation models in the light of self-interacting sterile neutrinos*, *Phys. Rev. D* **101** (2020), no. 8 083521, [[arXiv:1911.08512](#)].
- [7] N. Blinov and G. Marques-Tavares, *Interacting radiation after Planck and its implications for the Hubble Tension*, *JCAP* **09** (2020) 029, [[arXiv:2003.08387](#)].
- [8] H.-J. He, Y.-Z. Ma, and J. Zheng, *Resolving Hubble Tension by Self-Interacting Neutrinos with Dirac Seesaw*, *JCAP* **11** (2020) 003, [[arXiv:2003.12057](#)].
- [9] A. Das, A. Dighe, and M. Sen, *New effects of non-standard self-interactions of neutrinos in a supernova*, *JCAP* **05** (2017) 051, [[arXiv:1705.00468](#)].
- [10] H. Ko et al., *Neutrino Process in Core-collapse Supernovae with Neutrino Self-interaction and MSW Effects*, *Astrophys. J. Lett.* **891** (2020), no. 1 L24.
- [11] K. Blum, A. Hook, and K. Murase, *High energy neutrino telescopes as a probe of the neutrino mass mechanism*, [arXiv:1408.3799](#).
- [12] N. Blinov, K. J. Kelly, G. Z. Krnjaic, and S. D. McDermott, *Constraining the Self-Interacting Neutrino Interpretation of the Hubble Tension*, *Phys. Rev. Lett.* **123** (2019), no. 19 191102, [[arXiv:1905.02727](#)].
- [13] V. Brdar, M. Lindner, S. Vogl, and X.-J. Xu, *Revisiting neutrino self-interaction constraints from  $Z$  and  $\tau$  decays*, *Phys. Rev. D* **101** (2020), no. 11 115001, [[arXiv:2003.05339](#)].
- [14] K. C. Y. Ng and J. F. Beacom, *Cosmic neutrino cascades from secret neutrino interactions*, *Phys. Rev. D* **90** (2014), no. 6 065035, [[arXiv:1404.2288](#)]. [Erratum: *Phys. Rev. D* **90**, 089904 (2014)].
- [15] A. DiFranzo and D. Hooper, *Searching for MeV-Scale Gauge Bosons with IceCube*, *Phys. Rev. D* **92** (2015), no. 9 095007, [[arXiv:1507.03015](#)].
- [16] I. M. Shoemaker and K. Murase, *Probing BSM Neutrino Physics with Flavor and Spectral Distortions: Prospects for Future High-Energy Neutrino Telescopes*, *Phys. Rev. D* **93** (2016), no. 8 085004, [[arXiv:1512.07228](#)].
- [17] M. Bustamante, C. Rosenstrøm, S. Shalgar, and I. Tamborra, *Bounds on secret neutrino interactions from high-energy astrophysical neutrinos*, *Phys. Rev. D* **101** (2020), no. 12 123024, [[arXiv:2001.04994](#)].
- [18] **Planck** Collaboration, N. Aghanim et al., *Planck 2018 results. VI. Cosmological parameters*, [arXiv:1807.06209](#).
- [19] G. Efstathiou,  *$H_0$  Revisited*, *Mon. Not. Roy. Astron. Soc.* **440** (2014), no. 2 1138–1152, [[arXiv:1311.3461](#)].
- [20] J. L. Bernal, L. Verde, and A. G. Riess, *The trouble with  $H_0$* , *JCAP* **10** (2016) 019, [[arXiv:1607.05617](#)].
- [21] L. Verde, T. Treu, and A. Riess, *Tensions between the early and late universe*, *Nature Astronomy* **03** (Sep, 2019) 891–895, [[arXiv:1907.10625](#)].
- [22] E. Di Valentino et al., *Cosmology Intertwined II: The Hubble Constant Tension*, [arXiv:2008.11284](#).
- [23] A. G. Riess, S. Casertano, W. Yuan, L. M. Macri, and D. Scolnic, *Large Magellanic Cloud Cepheid Standards Provide a 1% Foundation for the Determination of the Hubble Constant and Stronger Evidence for Physics beyond  $\Lambda$ CDM*, *Astrophys. J.* **876** (2019), no. 1 85, [[arXiv:1903.07603](#)].

- [24] K.-F. Lyu, E. Stamou, and L.-T. Wang, *Self-interacting neutrinos: solution to Hubble tension versus experimental constraints*, [arXiv:2004.10868](#).
- [25] F. F. Deppisch, L. Graf, W. Rodejohann, and X.-J. Xu, *Neutrino Self-Interactions and Double Beta Decay*, *Phys. Rev. D* **102** (2020), no. 5 051701, [[arXiv:2004.11919](#)].
- [26] K. Ioka and K. Murase, *IceCube PeV–EeV neutrinos and secret interactions of neutrinos*, *PTEP* **2014** (2014), no. 6 061E01, [[arXiv:1404.2279](#)].
- [27] B. Chauhan and S. Mohanty, *Signature of light sterile neutrinos at IceCube*, *Phys. Rev. D* **98** (2018), no. 8 083021, [[arXiv:1808.04774](#)].
- [28] K. J. Kelly and P. A. Machado, *Multimessenger Astronomy and New Neutrino Physics*, *JCAP* **10** (2018) 048, [[arXiv:1808.02889](#)].
- [29] S. Mohanty, A. Narang, and S. Sadhukhan, *Cutoff of IceCube Neutrino Spectrum due to  $t$ -channel Resonant Absorption by  $C\nu B$* , *JCAP* **03** (2019) 041, [[arXiv:1808.01272](#)].
- [30] C. Creque-Sarbinowski, J. Hyde, and M. Kamionkowski, *Resonant Neutrino Self-Interactions*, [arXiv:2005.05332](#).
- [31] Y. Chikashige, R. N. Mohapatra, and R. Peccei, *Are There Real Goldstone Bosons Associated with Broken Lepton Number?*, *Phys. Lett. B* **98** (1981) 265–268.
- [32] G. Gelmini and M. Roncadelli, *Left-Handed Neutrino Mass Scale and Spontaneously Broken Lepton Number*, *Phys. Lett. B* **99** (1981) 411–415.
- [33] H. M. Georgi, S. L. Glashow, and S. Nussinov, *Unconventional Model of Neutrino Masses*, *Nucl. Phys. B* **193** (1981) 297–316.
- [34] G. B. Gelmini, S. Nussinov, and M. Roncadelli, *Bounds and Prospects for the Majoron Model of Left-handed Neutrino Masses*, *Nucl. Phys. B* **209** (1982) 157–173.
- [35] S. Nussinov and M. Roncadelli, *Observable Effects of Relic Majorons*, *Phys. Lett. B* **122** (1983) 387–391.
- [36] U. K. Dey, N. Nath, and S. Sadhukhan, *Charged Higgs effects in IceCube: PeV events and NSIs*, [arXiv:2010.05797](#).
- [37] F. Arias-Aragon, E. Fernandez-Martinez, M. Gonzalez-Lopez, and L. Merlo, *Neutrino Masses and Hubble Tension via a Majoron in MFV*, [arXiv:2009.01848](#).
- [38] M. Berbig, S. Jana, and A. Trautner, *The Hubble tension and a renormalizable model of gauged neutrino self-interactions*, [arXiv:2004.13039](#).
- [39] I. Esteban, M. Gonzalez-Garcia, M. Maltoni, T. Schwetz, and A. Zhou, *The fate of hints: updated global analysis of three-flavor neutrino oscillations*, [arXiv:2007.14792](#).
- [40] H. Goldberg, G. Perez, and I. Sarcevic, *Mini  $Z'$  burst from relic supernova neutrinos and late neutrino masses*, *JHEP* **11** (2006) 023, [[hep-ph/0505221](#)].
- [41] Y. Farzan and S. Palomares-Ruiz, *Dips in the Diffuse Supernova Neutrino Background*, *JCAP* **06** (2014) 014, [[arXiv:1401.7019](#)].
- [42] C.-P. Ma and E. Bertschinger, *Cosmological perturbation theory in the synchronous and conformal Newtonian gauges*, *Astrophys. J.* **455** (1995) 7–25, [[astro-ph/9506072](#)].
- [43] S. Hannestad and R. J. Scherrer, *Selfinteracting warm dark matter*, *Phys. Rev. D* **62** (2000) 043522, [[astro-ph/0003046](#)].
- [44] F. Forastieri, M. Lattanzi, G. Mangano, A. Mirizzi, P. Natoli, and N. Saviano, *Cosmic microwave background constraints on secret interactions among sterile neutrinos*, *JCAP* **07** (2017) 038, [[arXiv:1704.00626](#)].
- [45] N. Song, M. Gonzalez-Garcia, and J. Salvado, *Cosmological constraints with self-interacting sterile neutrinos*, *JCAP* **10** (2018) 055, [[arXiv:1805.08218](#)].



- [46] J. Lesgourgues, *The Cosmic Linear Anisotropy Solving System (CLASS) I: Overview*, [arXiv:1104.2932](#).
- [47] B. Audren, J. Lesgourgues, K. Benabed, and S. Prunet, *Conservative Constraints on Early Cosmology: an illustration of the Monte Python cosmological parameter inference code*, *JCAP* **1302** (2013) 001, [[arXiv:1210.7183](#)].
- [48] **Planck** Collaboration, Y. Akrami et al., *Planck 2018 results. X. Constraints on inflation*, [arXiv:1807.06211](#).
- [49] **BOSS** Collaboration, S. Alam et al., *The clustering of galaxies in the completed SDSS-III Baryon Oscillation Spectroscopic Survey: cosmological analysis of the DR12 galaxy sample*, *Mon. Not. Roy. Astron. Soc.* **470** (2017), no. 3 2617–2652, [[arXiv:1607.03155](#)].
- [50] A. Lewis, *GetDist: a Python package for analysing Monte Carlo samples*, [arXiv:1910.13970](#).
- [51] M. Ahlers, L. A. Anchordoqui, and S. Sarkar, *Neutrino diagnostics of ultra-high energy cosmic ray protons*, *Phys. Rev. D* **79** (2009) 083009, [[arXiv:0902.3993](#)].
- [52] S. Ando and K. Sato, *Relic neutrino background from cosmological supernovae*, *New J. Phys.* **6** (2004) 170, [[astro-ph/0410061](#)].
- [53] S. Horiuchi, J. F. Beacom, and E. Dwek, *The Diffuse Supernova Neutrino Background is detectable in Super-Kamiokande*, *Phys. Rev. D* **79** (2009) 083013, [[arXiv:0812.3157](#)].
- [54] **IceCube** Collaboration, C. Kopper, *Observation of Astrophysical Neutrinos in Six Years of IceCube Data*, *PoS ICRC2017* (2018) 981.
- [55] W. Hastings, *Monte Carlo Sampling Methods Using Markov Chains and Their Applications*, *Biometrika* **57** (1970) 97–109.
- [56] R. Barlow, *Asymmetric statistical errors*, in *Statistical Problems in Particle Physics, Astrophysics and Cosmology*, pp. 56–59, 6, 2004. [physics/0406120](#).